

# MOTS-c accelerates bone fracture healing by stimulating osteogenesis of bone marrow mesenchymal stem cells *via* positively regulating FOXF1 to activate the TGF- $\beta$ pathway

F.-B. WENG, L.-F. ZHU, J.-X. ZHOU, Y. SHAN, Z.-G. TIAN, L.-W. YANG

Department of Orthopedics, The Ninth People's Hospital of Suzhou, Suzhou, China

Fengbiao Weng and Lifan Zhu contributed equally to this work

**Abstract.** – **OBJECTIVE:** To elucidate the function of MOTS-c in accelerating bone fracture healing by inducing BMSCs differentiation into osteoblasts, as well as its potential mechanism.

**MATERIALS AND METHODS:** Primary BMSCs were extracted from rats and induced for osteogenesis. The highest dose of MOTS-c that did not affect BMSCs proliferation was determined by CCK-8 assay. After 7-day osteogenesis, the relative levels of ALP, Bglap, and Runx2 in MOTS-c-treated BMSCs influenced by FOXF1 were examined. ALP staining and Alizarin red staining in BMSCs were performed as well. The interaction between FOXF1 and TGF- $\beta$  was analyzed by ChIP assay. In addition, rescue experiments were performed to investigate the role of FOXF1/TGF- $\beta$  axis in MOTS-c-induced osteogenesis.

**RESULTS:** 1  $\mu$ M MOTS-c was the highest dose that did not affect BMSCs proliferation. MOTS-c treatment upregulated relative levels of ALP, Bglap, and Runx2, and stimulated mineralization ability of BMSCs, which were attenuated by the silence of FOXF1. TGF- $\beta$  was proved to interact with FOXF1 and its level was positively mediated by FOXF1. The silence of FOXF1 attenuated MOTS-c accelerated osteogenesis and TGF- $\beta$  upregulation in BMSCs because of MOTS-c induction, and these trends were further reversed by the overexpression of TGF- $\beta$ .

**CONCLUSIONS:** MOTS-c treatment markedly induces osteogenesis in BMSCs. During MOTS-c-induced osteogenic progression, the upregulated FOXF1 triggers the activation of TGF- $\beta$  pathway, thus accelerating bone fracture healing.

*Key Words:*

MOTS-c, BMSCs, Osteogenesis, TGF- $\beta$ .

## Introduction

Fracture is the most common traumatic injury in humans. Fracture healing is an acquired regeneration process involving embryonic bone development<sup>1</sup>. Risk factors for nonunion of the fracture include malnutrition, infection, metabolic diseases, vascularization, or vascular injury<sup>2</sup>. The role of cellular dysfunction in the pathogenesis of fracture nonunion remains unclear.

Bone mesenchymal stem cells (BMSCs) are the stem cells present in the bone marrow stroma<sup>1,2</sup>. BMSCs have been extensively studied in clinical trials, and they could be used in the treatment of myocardial infarction, osteogenesis imperfecta, osteoarthritis, and tissue repair<sup>3</sup>. Many reports<sup>4-7</sup> have shown a promising application of BMSCs in the treatment of fracture nonunion. Although the importance of BMSCs in osteogenesis is well concerned, molecular mechanisms underlying BMSCs in fracture healing are required for further explorations.

MOTS-c is a 16-amino-acid peptide encoded by the mitochondrial open reading frame of the 12S rRNA-c<sup>8</sup>. Mitochondrial-derived peptides (MOTS-c) are secreted into the blood and exert their functions in cell-autonomous and hormonal ways<sup>9</sup>. Previous investigations<sup>10</sup> have demonstrated the capacities of MOTS-c to stimulate proliferation, differentiation, and mineralization and to inhibit apoptosis of osteoblasts, thus influencing the progression of osteogenesis. This paper mainly clarified the role of MOTS-C in BMSCs osteogenesis and its specific mechanism.

## Materials and Methods

### **BMSCs Isolation and Cell Culture**

28-35-day-old rats with 80-100 g were sacrificed and immersed in 75% ethanol for 10 min. Bilateral femora of rats were extracted and immersed in PBS. Bone marrow cavity of the femur was repeatedly washed by culture medium. The mixture containing bone marrow cavity contents was centrifuged, and the precipitant was cultured in a 5% CO<sub>2</sub> humidified incubator at 37°C. The culture medium was completely replaced after 48 h. The cell passage was performed until 80-90% confluence. Growth condition, morphology, and differentiation of BMSCs were observed under a microscope.

Ordinary medium: Dulbecco's Modified Eagle's Medium (DMEM; Thermo Fisher Scientific, Waltham, MA, USA) + 10% fetal bovine serum (FBS; Gibco, Rockville, MD, USA), + 1% penicillin-streptomycin.

Osteoinduce medium: Ordinary medium + 10 mmol/L  $\beta$ -glycerophosphate + 50  $\mu$ g/ml ascorbic acid.

### **Quantitative Real Time-Polymerase Chain Reaction (qRT-PCR)**

The total RNA of BMSCs was extracted by TRIzol (Invitrogen, Carlsbad, CA, USA) method followed by measurement of RNA concentration using an ultraviolet spectrophotometer (Hitachi, Tokyo, Japan). The complementary DNA (cDNA) synthesis and according to the instructions of the PrimeScript™ RT MasterMix kit (Invitrogen, Carlsbad, CA, USA). QRT-PCR reaction conditions were as follows: 94°C for 30 s, 55°C for 30 s, and 72°C for 90 s, for a total of 40 cycles. The relative level of the target gene was expressed by the 2<sup>- $\Delta\Delta$ CT</sup> method. GAPDH was served as the internal control. The primer sequences were listed as follows: ALP, F: 5'-AGGCTTCTTCTTGCTGGTG-3', R: 5'-GTTACCCTTATGATGTCC-3'; Bglap, F: 5'-AGTAAAGTGCAGCCTTTGT-3', R: 5'-GCCCCTTCTTCACT-3'; Runx2, F: 5'-CTTCCTCGCTCCGTGCTG-3', R: 5'-TCCTGCTGCTGCTGCTGCTG-3'; TGF- $\beta$ , F: 5'-GTAAGCTGATGAGTGCAATGAC-3', R: 5'-CAGATATGGCAACTCCCAGTG-3'; GAPDH, F: 5'-AGGTCGGTGTGAACGGATTTC-3', R: 5'-TGTAGACCATGTAGTTGAGGTCA-3'

### **Cell Transfection**

Third-generation BMSCs were cultured at 60% confluence and subjected to cell transfection

using Lipofectamine 2000. The medium was replaced at 6 h. The transfected cells for 48 h were harvested for subsequent experiments.

### **Cell Counting Kit (CCK-8)**

BMSCs were inoculated in a 96-well plate and cultured for 24 h. On the next day, the culture medium was replaced. For assessing cell viability, 10  $\mu$ l of CCK-8 was added in each well. After 1-h incubation, absorbance at 450 nm was determined using a microplate reader.

### **ALP Staining**

After osteogenic differentiation of BMSCs for 14 days, the cells seeded on slices that were inserted in a 6-well plate were treated with incubation buffer of 3%  $\beta$ -glycerophosphate + 5 ml of 2% barbitone sodium + 10 ml of distilled water + 10 ml of 2% calcium chloride + 1 ml of 2% magnesium sulfate at 37°C for 15 min. Subsequently, the cells were washed with PBS for 2 min and counterstained with hematoxylin for 5 min. Finally, the cells were captured under an inverted microscope.

### **Alizarin Red Staining (ARS)**

For osteogenic differentiation of BMSCs for 14 days, the cells were washed with PBS for three times, fixed in 60% isopropanol for 60 s, and washed with PBS twice for 2 min. Subsequently, BMSCs were subjected to 1% ARS staining for 5 min. Calcified nodules were observed and captured using an inverted microscope.

### **ChIP**

Chromatin immunoprecipitation (ChIP) was performed using the Magna ChIP A/G Kit (Millipore, Bedford, MA). Chromatin immunoprecipitated DNA was eluted, reversely X-linked, purified, and subjected to qRT-PCR.

### **Western Blot**

The total protein from BMSCs was extracted using radioimmunoprecipitation assay (RIPA; Beyotime, Shanghai, China). The BCA (bicinchoninic acid) method was performed to quantitate the protein concentration. The protein samples were electrophoresed on polyacrylamide gels and then transferred to polyvinylidene difluoride (PVDF) membranes (Merck Millipore, Billerica, MA, USA). After blocking with 5% skimmed milk, the membranes were incubated with primary antibody (Cell Signaling Technology, Danvers, MA, USA) at 4°C overnight. The membrane

was incubated with the secondary antibody after rinsing with the buffer solution (TBST). The bands were exposed by ECL, and the grey values were analyzed by Image Software.

### Statistical Analysis

The Statistical Product and Service Solution 16.0 (SPSS Inc., Chicago, IL, USA) was used for all statistical analysis. The data were expressed as mean  $\pm$  SD. The *t*-test was used to analyze the differences between the two groups.  $p < 0.05$  indicated a significant difference.

## Results

### MOTS-c Stimulated BMSCs Osteogenesis

BMSCs were treated with different doses of MOTS-c (0, 0.5, 1, 1.5, and 2  $\mu$ M) for 24 h. Viability in BMSCs was not altered under the treatment of 0.5 and 1  $\mu$ M MOTS-c, while cell viability was markedly elevated after treatment of 1.5 and 2  $\mu$ M MOTS-c (Figure 1A). Therefore, 1  $\mu$ M MOTS-c was the highest dose that did not affect BMSCs proliferation and it was adopted in the following experiments. After 1  $\mu$ M MOTS-c

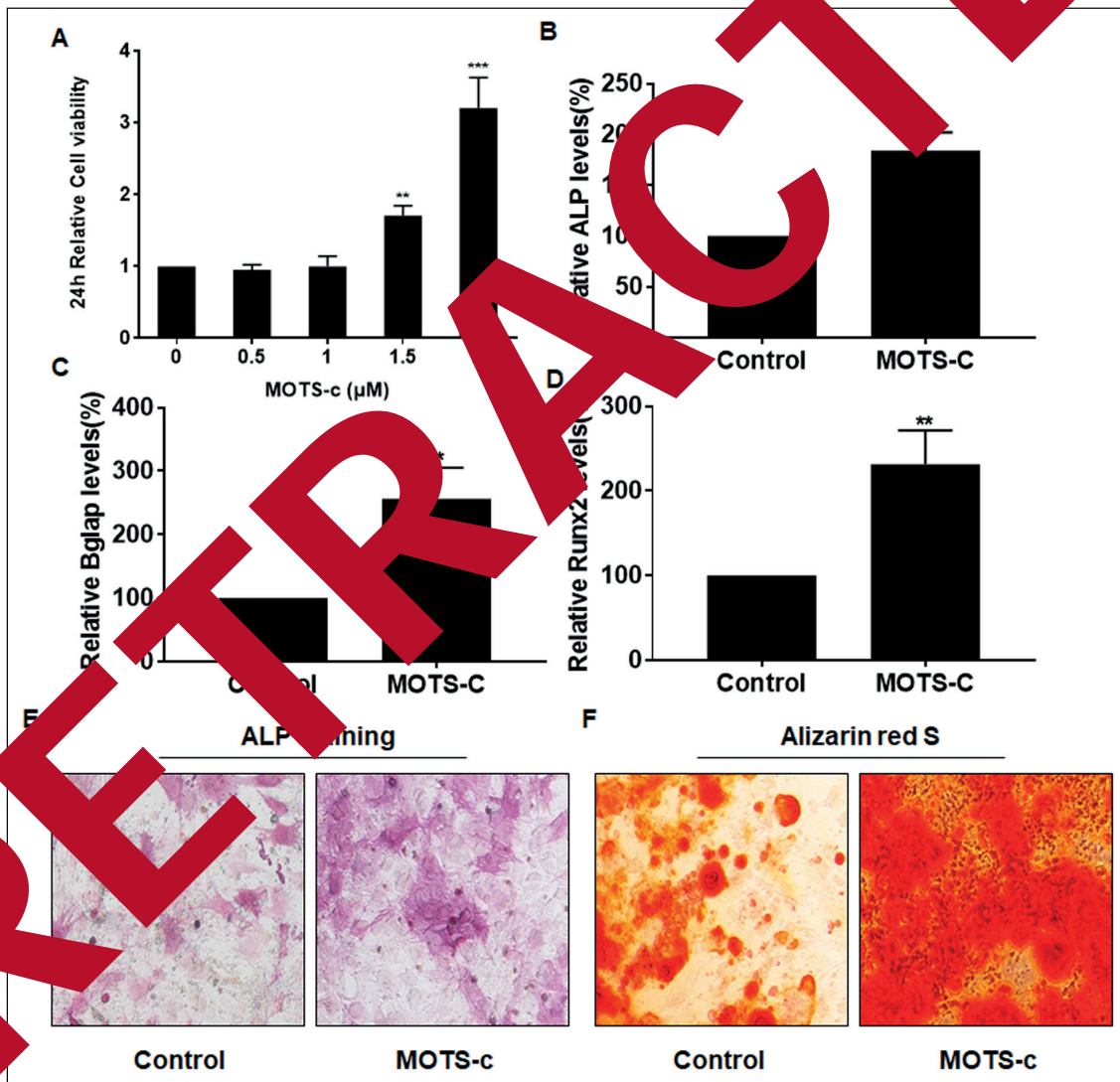


**Figure 1.** MOTS-c stimulated BMSCs osteogenesis. **A**, Viability in BMSCs treated with 0, 0.5, 1, 1.5, and 2  $\mu$ M MOTS-c for 24 h. **B**, ALP level in BMSCs either treated with 1  $\mu$ M MOTS-c or not. **C**, Bglap level in BMSCs either treated with 1  $\mu$ M MOTS-c or not. **D**, Runx2 level in BMSCs either treated with 1  $\mu$ M MOTS-c or not. **E**, ALP staining in BMSCs either treated with 1  $\mu$ M MOTS-c or not (magnification: 100  $\times$ ). **F**, Alizarin red S staining in BMSCs either treated with 1  $\mu$ M MOTS-c or not (magnification: 100  $\times$ ).

treatment and osteogenic induction for 7 days, the relative levels of ALP, Bglap, and Runx2 were remarkably upregulated (Figure 1B-1D). ALP staining also revealed the enhanced ALP activity in MOTS-c-treated BMSCs (Figure 1E). After MOTS-c treatment, the number and volume of the mineralized nodules were elevated compared with those of controls (Figure 1F). The above data demonstrated the capacity of MOTS-c to induce BMSCs osteogenesis.

### **MOTS-c Stimulated BMSCs Osteogenesis via FOXF1**

After osteogenic induction for 7 days, FOXF1 level was markedly upregulated in BMSCs (Figure

2A). To uncover the biological role of FOXF1 in BMSCs osteogenesis, si-FOXF1 was constructed. The transfection of si-FOXF1 greatly downregulated FOXF1 level in MOTS-c-treated BMSCs. Interestingly, the transfection of si-FOXF1 blocked the upregulation of ALP, Bglap, and Runx2 in BMSCs treated with MOTS-c (Figure 2B-2D). Hence, it is believed that MOTS-c stimulated BMSCs osteogenesis by upregulating FOXF1.

### **FOXF1 Regulated the TGF- $\beta$ Pathway**

TGF- $\beta$  pathway is one of the important regulatory pathways in BMSCs during the differentiation of BMSCs into osteoblasts<sup>11</sup>. ChIP assay

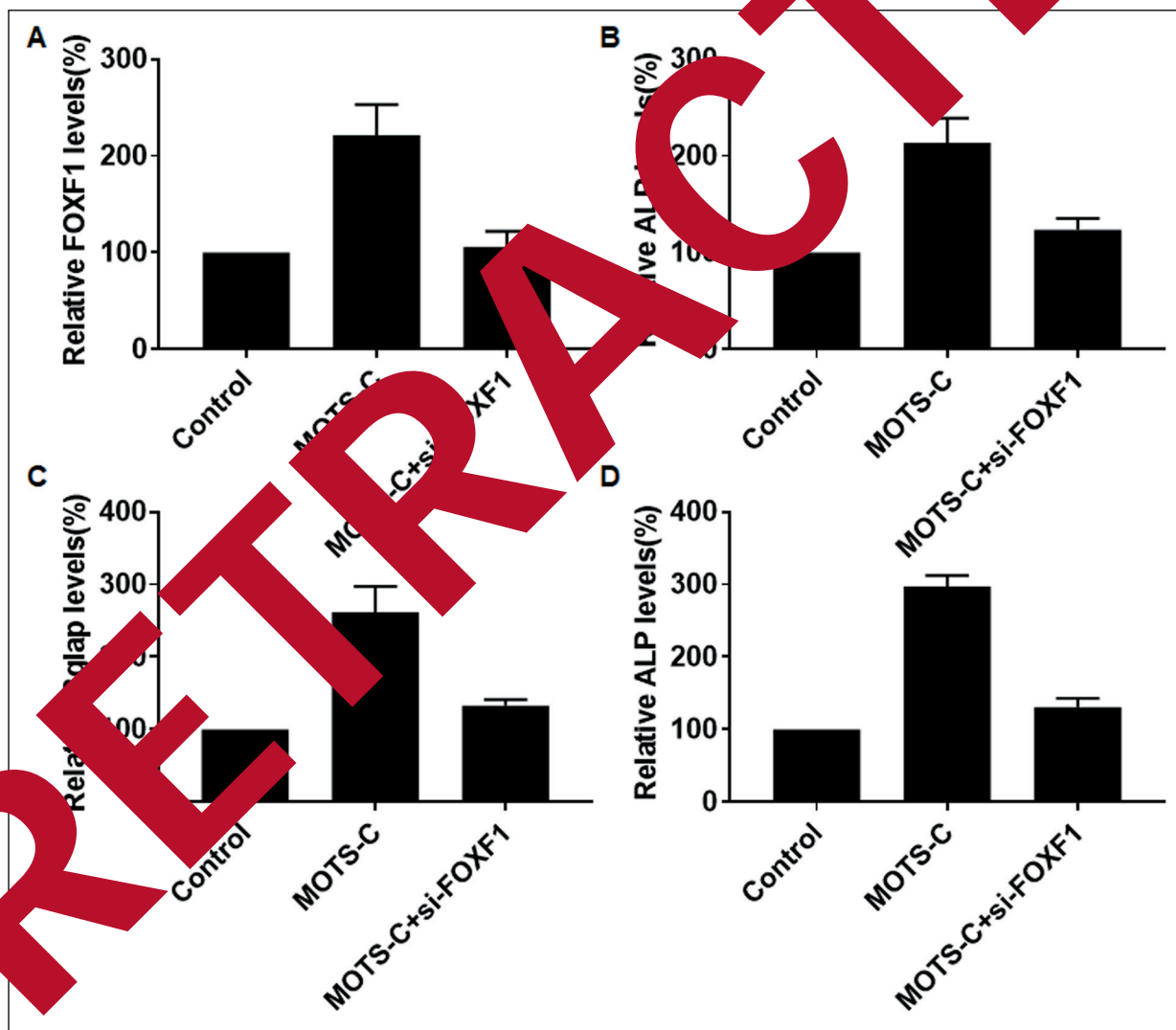


**Figure 2.** MOTS-c stimulated BMSCs osteogenesis *via* FOXF1. BMSCs were treated with blank control, 1  $\mu$ M MOTS-c, or 1  $\mu$ M MOTS-c and si-FOXF1 transfection. The relative levels of FOXF1 (A), ALP (B), Bglap (C), and Runx2 (D) in BMSCs were determined.



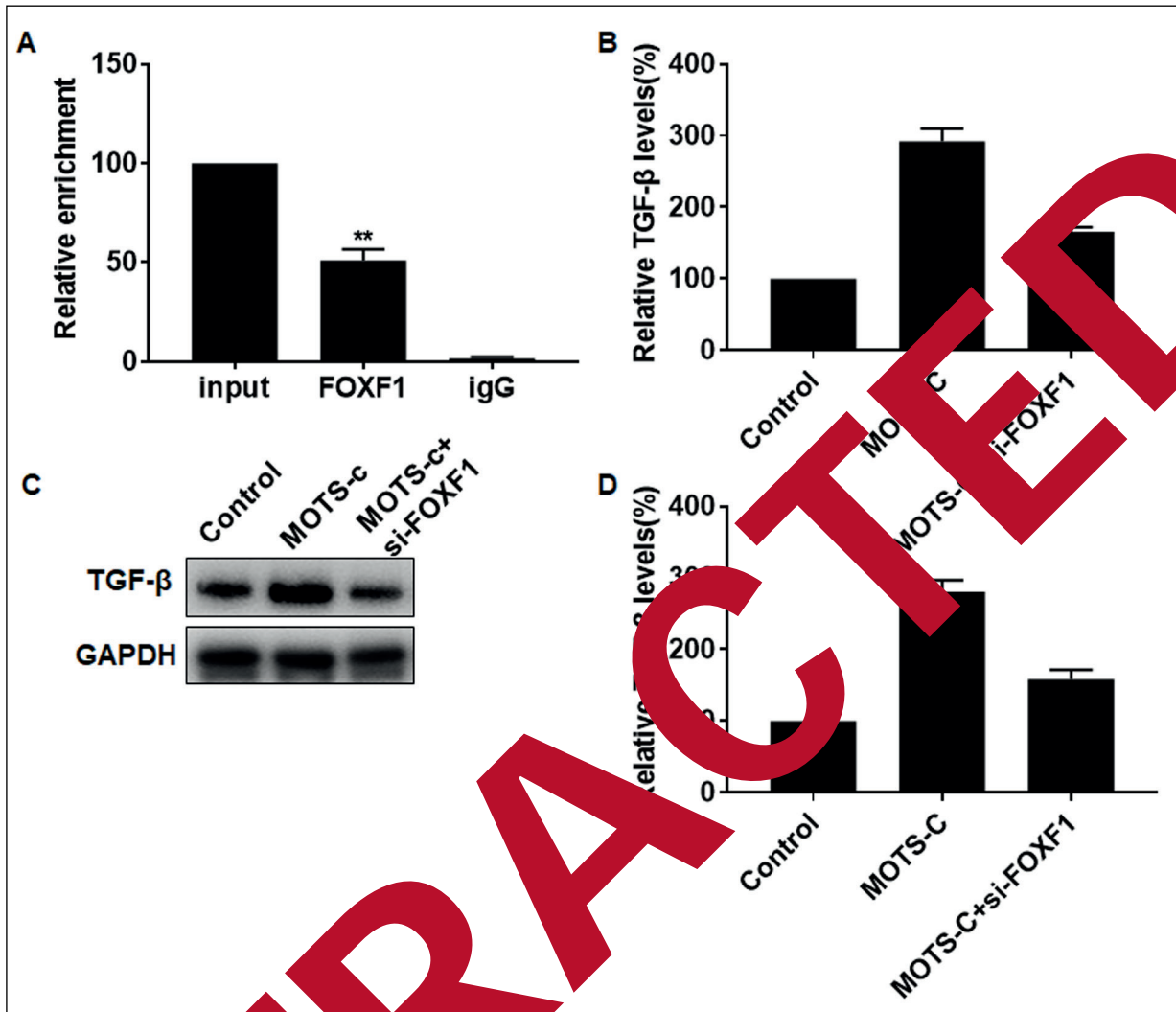


**Figure 3.** FOXF1 regulated the TGF- $\beta$  pathway. **A**, Relative enrichment of TGF- $\beta$  in input, anti-FOXF1, and anti-IgG. BMSCs were treated with 1  $\mu$ M control, 1  $\mu$ M MOTS-c, or 1  $\mu$ M MOTS-c, and si-FOXF1 transfection. The mRNA (**B**) and protein (**C**, **D**) levels of TGF- $\beta$  in BMSCs were determined.

revealed a higher enrichment of TGF- $\beta$  in anti-FOXF1 than that in anti-IgG, verifying that FOXF1 could bind to the promoter region of TGF- $\beta$  and that FOXF1 stimulate its transcription (Figure 3A). TGF- $\beta$  level was upregulated during MOTS-c-induced osteogenesis in BMSCs, which was downregulated by the transfection of si-FOXF1 (Figure 3B-3D).

#### **FOXF1 Stimulated BMSCs Osteogenesis Through the TGF- $\beta$ Pathway**

A previous study has confirmed that the silence of FOXF1 reversed the accelerated osteogenesis and TGF- $\beta$  upregulation in MOTS-c-treated

BMSCs. It is noteworthy that the downregulated TGF- $\beta$  in MOTS-c-treated BMSCs transfected with si-FOXF1 was partially reversed after the co-transfection of pcDNA-TGF- $\beta$  (Figure 4A). Similarly, downregulated ALP, Bglap, and Runx2 levels in MOTS-c-treated BMSCs with FOXF1 knockdown were elevated after the overexpression of TGF- $\beta$  (Figure 4B-4D). ALP staining showed the same trend in ALP activity as that of the ALP level (Figure 4E). Mineralization ability was reversed by TGF- $\beta$  overexpression (Figure 4F). As a result, MOTS-c stimulated BMSCs osteogenesis through FOXF1 to activate the TGF- $\beta$  pathway.

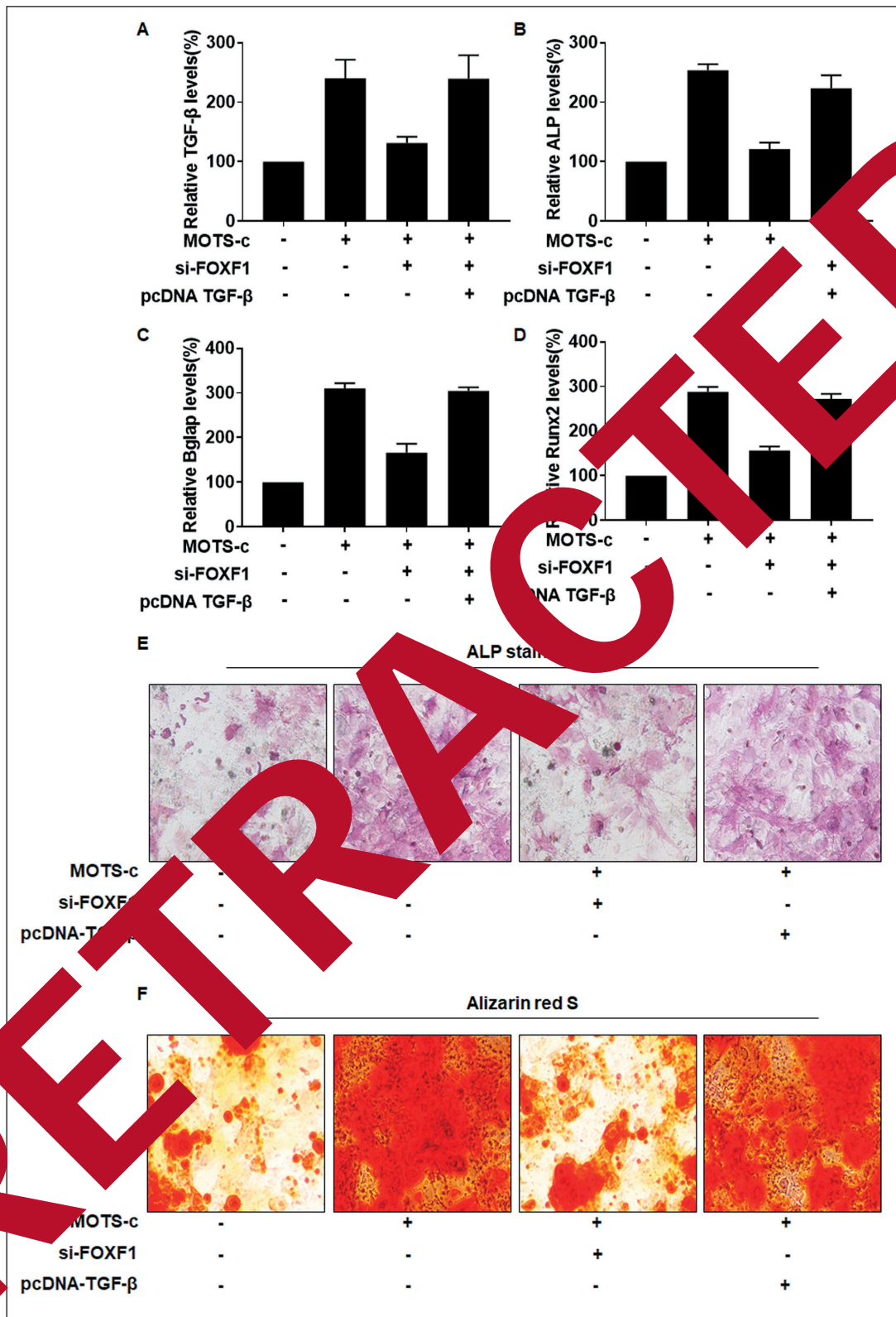


**Figure 4.** FOXF1 stimulated BMSCs osteogenesis through the TGF-β pathway. BMSCs were treated with blank control, MOTS-c treatment, MOTS-c treatment + si-FOXF1 transfection, or MOTS-c treatment + co-transfection of si-FOXF1 and pcDNA-TGF-β. The relative levels of FOXF1 (A), ALP (B), Bglap (C), and Runx2 (D) in BMSCs were determined. ALP activity (E) and mineralization ability (F) were assessed by ALP staining and Alizarin red S staining, respectively (magnification: 100 ×).

## Discussion

Mammalian bones can be rejuvenated or regenerated after bone injury. It is a complex process involving immune responses and synergy of osteoclasts and osteoblasts<sup>12</sup>. Self-renewal, multi-directional differentiation, and migration of BMSCs are key factors affecting fracture healing<sup>3</sup>.

It is reported that MOTS-c in mouse bone tissues is able to prevent osteoporosis<sup>13</sup>. As key genes involving in osteogenesis, ALP, Bglap, and Runx2 levels influenced by MOTS-c were examined in this experiment<sup>12</sup>. Our results showed that MOTS-c treatment upregulated mRNA levels of ALP, Bglap, and Runx2 in BMSCs. Moreover, MOTS-c treatment greatly enhanced the mineralization ability, suggesting the osteogenic potential of MOTS-c.

Forkhead box F1 (FOXF1) belongs to the FOX transcription factor family. It contains a highly conserved DNA binding region (DBD)<sup>14</sup>. FOXF1 is a key regulator of embryonic development. It is reported<sup>15-17</sup> that FOXF1 deficiency leads to various developmental abnormalities and lethality. FOXF1 is also required for regeneration after lung injury<sup>18</sup>. Our results found that the silencing of FOXF1 in BMSCs could block MOTS-c-induced upregulation in ALP, Bglap, and Runx2, verifying that FOXF1 was responsible for BMSC osteogenesis.

As a crucial multifunctional cytokine, TGF- $\beta$  is able to regulate embryogenesis, homeostasis, and cellular behavior. The vital function of TGF- $\beta$  in BMSCs osteogenesis has already been identified. Wang et al. pointed out that Smad3, an intracellular effector of TGF- $\beta$ , is activated and translocated into the nucleus, where it modulates the expression level of Runx2. Here, the interaction between FOXF1 and TGF- $\beta$  was confirmed by CHIP assay. Moreover, TGF- $\beta$  level was positively regulated by FOXF1. The silencing of FOXF1 attenuated osteogenesis induced by MOTS-c treatment, which was further reversed by overexpression of TGF- $\beta$ . Collectively, MOTS-c induced BMSCs osteogenesis through FOXF1 to activate the TGF- $\beta$  pathway.

## Conclusions

In this study, we first observed that MOTS-c treatment markedly induces osteogenesis in BMSCs. During MOTS-c-induced osteogenic pro-

gression, FOXF1 is upregulated and triggers the activation of TGF- $\beta$  pathway, thus accelerating bone fracture healing.

## Conflict of Interest

The Authors declare that they have no conflict of interests.

## References

- 1) CAI X, YANG F, YAN X, LI W, YU M, OORTGIESEN J, WANG Y, JANSEN JA, VAN DER MEER LF. Influence of bone marrow-derived mesenchymal stem cells pre-implanted and differentiated on periodontal regeneration in vivo. *J Periodontol* 2015; 46: 130-137.
- 2) SEEBACH C, HENRICH J, WYKSBURY R, WILHELM K, MARZI I. Number and proliferative capacity of human mesenchymal stem cells are modulated positively in multiple trauma patients and negatively in atrophic nonunions. *Calcif Tissue Int* 2007; 80: 294-300.
- 3) SUN P, JIA K, ZHANG C, ZHU X, LI J, HE L, SIWKO S, XUE LIU M, LUO W. Loss of Lgr4 inhibits differentiation, migration and apoptosis, and promotes proliferation of bone mesenchymal stem cells. *J Cell Physiol* 2019; 234: 10855-10867.
- 4) MARCACCI M, KON E, MUKHACHEV V, LAVROUKOV A, KUTEPOV QUARTO R, MASTROGIACOMO M, CANCEDDA R. Stem cells associated with macroporous bioceramics for long bone repair: 6- to 7-year outcome of a pilot clinical study. *Tissue Eng* 2007; 13: 947-955.
- 5) QUARTO R, MASTROGIACOMO M, CANCEDDA R, KUTEPOV SM, MUKHACHEV V, LAVROUKOV A, KON E, MARCACCI M. Repair of large bone defects with the use of autologous bone marrow stromal cells. *N Engl J Med* 2001; 344: 385-386.
- 6) HERNIGOU P, MATHIEU G, POIGNARD A, MANICOM O, BEAUJEUAN F, ROUARD H. Percutaneous autologous bone-marrow grafting for nonunions. Surgical technique. *J Bone Joint Surg Am* 2006; 88 Suppl 1 Pt 2: 322-327.
- 7) HERNIGOU P, POIGNARD A, MANICOM O, MATHIEU G, ROUARD H. The use of percutaneous autologous bone marrow transplantation in nonunion and avascular necrosis of bone. *J Bone Joint Surg Br* 2005; 87: 896-902.
- 8) LEE C, KIM KH, COHEN P. MOTS-c: a novel mitochondrial-derived peptide regulating muscle and fat metabolism. *Free Radic Biol Med* 2016; 100: 182-187.
- 9) LU H, WEI M, ZHAI Y, LI Q, YE Z, WANG L, LUO W, CHEN J, LU Z. MOTS-c peptide regulates adipose homeostasis to prevent ovariectomy-induced metabolic dysfunction. *J Mol Med (Berl)* 2019; 97: 473-485.
- 10) HU BT, CHEN WZ. MOTS-c improves osteoporosis by promoting osteogenic differentiation of bone marrow mesenchymal stem cells via TGF-be-

- ta/Smad pathway. *Eur Rev Med Pharmacol Sci* 2018; 22: 7156-7163.
- 11) CHE N, QIU W, WANG JK, SUN XX, XU LX, LIU R, GU L. MOTS-c improves osteoporosis by promoting the synthesis of type I collagen in osteoblasts via TGF-beta/SMAD signaling pathway. *Eur Rev Med Pharmacol Sci* 2019; 23: 3183-3189.
  - 12) LIU H, SU H, WANG X, HAO W. MiR-148a regulates bone marrow mesenchymal stem cells-mediated fracture healing by targeting insulin-like growth factor 1. *J Cell Biochem* 2018; doi: 10.1002/jcb.27121. [Epub ahead of print].
  - 13) MING W, LU G, XIN S, HUANYU L, YINGHAO J, XIAOYING L, CHENMING X, BANJUN R, LI W, ZIFAN L. Mitochondria related peptide MOTS-c suppresses ovariectomy-induced bone loss via AMPK activation. *Biochem Biophys Res Commun* 2016; 476: 412-419.
  - 14) WANG S, XIAO Z, HONG Z, JIAO H, ZHU S, ZHAO Y, BI J, QIU J, ZHANG D, YAN J, ZHANG L, HUANG C, LI T, LIANG L, LIAO W, YE Y, DING Y. FOXF1 promotes angiogenesis and accelerates bevacizumab resistance in colorectal cancer by transcriptionally activating VEGFA. *Cancer Lett* 2018; 439: 78-90.
  - 15) REN X, USTIYAN V, PRADHAN A, CAI Y, HAVRILAK JA, BOLTE CS, SHANNON JM, KALIN TV, KALINICHENKO VV. FOXF1 transcription factor is required for formation of embryonic vasculature by regulating VEGF signaling in endothelial cells. *Circ Res* 2014; 115: 709-720.
  - 16) NAGANO N, YOSHIKAWA K, HOSONO S, TAKAHASHI K, KAYAMA T. Alveolar capillary dysplasia with misalignment of the pulmonary veins due to nonsense insertion mutation of FOXF1. *Pediatr Int* 2016; 58: 1371-1372.
  - 17) LUK HM, TANG T, CHOY KW, TONG MF, WONG OK, LO FM. Maternal somatic mosaicism of FOXF1 mutation causes recurrent alveolar capillary dysplasia with misalignment of pulmonary veins in siblings. *Am J Med Genet A* 2016; 170: 1942-1944.
  - 18) BOLTE C, FLOOD HM, REN X, JAGANNATHAN S, BARSKA A, KALIN TV, KALINICHENKO VV. FOXF1 transcription factor promotes lung regeneration after partial pneumectomy. *Sci Rep* 2017; 7: 41109.
  - 19) WATANABE Y, ITOH S, GOTO T, OHNISHI E, YAMAMOTO M, ITOH F, SATOH K, WIERCINSKA E, YANG W, SHIMIZU NA, KAKIYAMA A, NAKANO N, MOMOI S AM, SHIBUYA H, KAWAKATSU K, KATO M. TMEPAI, a transmembrane TGF-beta-inducible protein, requires extracellular matrix proteins for active participation in TGF-beta signaling. *Mol Cell* 2010; 37: 123-134.
  - 20) CRANE JJ, LIU Y, CAO X. Role of TGF-beta signaling in coupling bone remodeling. *Methods Mol Biol* 2016; 1344: 281-297.
  - 21) DENG C, LI Y. TGF-beta and BMP signaling in osteoblast differentiation and bone formation. *Int J Biol Sci* 2012; 8: 272-288.
  - 22) WANG CL, XIAO Y, WANG CD, ZHU JF, SHEN C, ZUO W, WANG H, LIU W, WANG XY, FENG WJ, LI ZK, HU GL, LIU X, CHEN D. Gremlin2 suppression increases BMP2-induced osteogenesis of human bone marrow-derived mesenchymal stem cells via the BMP-2/Smad/Runx2 signaling pathway. *J Cell Biochem* 2017; 118: 286-297.